DESIGN AND ANALYSIS OF BUCK BOOST CONVERTER BASED LED DRIVER FOR ENHANCING THE STABILITY

Ramjee Prasad GUPTA
Department of Electrical Engineering, BIT,Sindri, Dhanbad, Jharkhand,India
Email : ramjee_gupta@yahoo.com
Dibya BHARTI
Department of Electrical Engineering, BIT,Sindri, Dhanbad, Jharkhand,India
Email :dibya_minu1@rediffmail.com
Dr. Upendra PRASAD
Department of Electrical Engineering, BIT,Sindri, Dhanbad, Jharkhand,India
Email :upendra_bit@yahoo.co.in

***Abstract**--This paper develops a light emitting diode (LED) driver circuit based on buck-boost converter including parasitic resistance. The transfer function analysis of buck boost converter and whole system has been obtained by considering parasitic resistance of the component because the resistance of an LED varies with temperature, making the circuit unstable. The forward bias of the LED used was 3.0V~4.5V, and the forward current was 0.6A. Ten 3W white-light LEDs were driven in series in the proposed circuit. In an LED only 15% to 25% of electrical energy is converted into light; the rest is converted into heat, which increases its temperature. In some typical application like designing of lighting system for underground coalmines this change in resistance can cause hazardous effect. Hence, LED must be operated at constant current for constant illumination for at least 10-12 hours without failure. Therefore, a closed-loop control system has been designed in this paper to increase output voltage stability. The driver circuit is operated in continuous buck-boost mode and the results are then simulated using PSIM software. The transfer function analysis has been done by using averaging method. For, stability analysis MATLAB and PSIM software has been used and it has been observed that phase margin is 93.8.º*

***Keywords**: buck-boost, closed-loop, stabilizer, LED, transfer function.*

1.INTRODUCTION

In general the power management of a LED can be divided into two main parts, namely, optimization of LED light output and efficient supply of power to the LED's. First, based on the LED characteristics and LED configuration different level of brightness could be obtained for the same amount of power. Hence, the term Luminous Efficiency which is defined as the ratio of luminous flux emitted from a light source to the electric power consumed by the source plays an important role governing overall efficiency. Second, an efficient conversion of the limited battery power to the useful form for LED's to emit proper amount of light is of significant importance. This conversion of power is often achieved using voltage regulators as LED drivers and present enormous system and circuit level issues which have been a topic of interest to the researchers [1][2][3]. In general, LED luminance is found to be directly proportional to its drive current [4] and hence in some applications like backlight, and flash the desired LED brightness is achieved by controlling the LED drive. Under the condition where desired brightness cannot be obtained using a single LED, additional LEDs can be placed either in parallel or series [5]. Low power LED has been used for battery powered applications for decades [6][7][8]. These applications include cell phone handsets, digital still cameras, automotive lighting, emergency lighting, and LCD backlighting, and so on. With the advancement of new materials and manufacture process, a new lighting source, that is, high brightness white (HBW) LED is now attracting more and more

attention from industry [9][10][11][12].This arrangement of multiple LEDs plays a significant role in defining the amount of current drained from the battery. In case of underground coalmines mine workers are very much dependent on visual cues to recognize underground mining hazards. On the other hand, illumination plays a critical role in miners' safety. Some hazards are located in the miners' peripheral field-of-view off-axis (10° to about 60°) or on-axis (0°)[13]. Closed-loop buck-boost converter for driving LED has been designed in which output voltage of 12 V has been maintained and it is independent of input voltage and load change[14].

2. Analysis of Buck Boost Converter

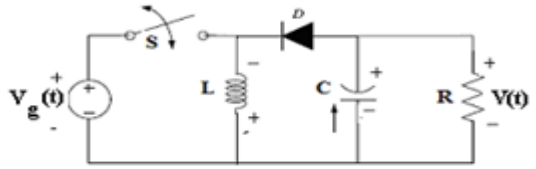

Figure1. Equivalent Circuit for Buck boost Converter

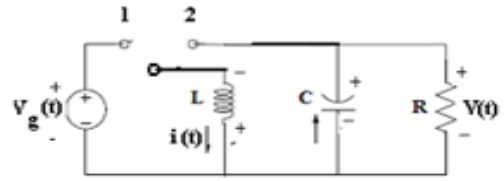

Figure 2. Equivalent Circuit for Buck boost Converter with switching operation

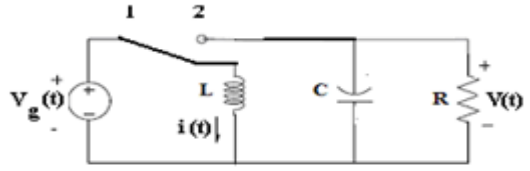

Figure 3. Buck boost Converter when switch is at position 1

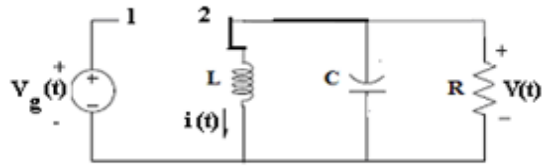

Figure 4 .Buck boost Converter when switch is at position 2

A simple method for deriving the small-signal ac model of CCM (continuous current mode) converters is explained by Averaging Method. The switching ripples in the inductor current and capacitor voltage waveforms are removed by averaging over one switching period. Hence, the low-frequency components of the inductor and capacitor waveforms are modelled by equations of the form

$$\begin{cases} L\frac{d\langle i_L(t)\rangle_{T_S}}{dt} = \langle v_L(t)\rangle_{T_s} \\ C\frac{d\langle v_c(t)\rangle_{T_S}}{dt} = \langle i_c(t)\rangle_{T_s} \end{cases} \quad (1)$$

Where $\langle x(t)\rangle T_s$ denotes the average of x(t) over an interval of length T_s.Let us derive a small-signal ac model of the buck-boost converter of Fig. 1.Let us consider R_L and R_C as the parasitic resistance of Inductor and capacitor respectively. The analysis begins as usual, by determining the voltage and current waveforms of the inductor and capacitor. When the switch is in position 1, the circuit of Fig. 3 is obtained. The inductor voltage and capacitor current are given by,

$$v_L(t) = L.\frac{di(t)}{dt} = v_g(t) - R_L.i(t) \quad (2)$$

$$i_C(t) = C.\frac{dv(t)}{dt} = -\frac{v(t)}{R+R_C} \quad (3)$$

We now make the small-ripple approximation. But rather than replacing $v_g(t)$ and $v(t)$ with their dc components V_g and V we now replace them with their low-frequency averaged values $\langle v_g(t)\rangle_{T_s}$ and $\langle v(t)\rangle_{T_s}$.Equations (2) and (3) becomes,

$$v_L(t) = L.\frac{di(t)}{dt} \approx \langle v_g(t)\rangle_{T_s} - R_L.\langle i(t)\rangle_{T_s} \quad (4)$$

$$i_C(t) = C.\frac{dv(t)}{dt} \approx -\frac{\langle v(t)\rangle_{T_S}}{R+R_C} \quad (5)$$

The inductor voltage and capacitor currents are

$$v_L(t) = L.\frac{di(t)}{dt} = v(t) - R_L.i(t) \quad (6)$$

$$i_C(t) = C.\frac{dv(t)}{dt} = -i(t) - \frac{v(t)}{R} \quad (7)$$

Using the small ripple approximation to replace i(t) and v(t) with their averaged values,

$$v_L(t) = L.\frac{di(t)}{dt} \approx \langle v(t)\rangle_{T_s} - R_L.\langle i(t)\rangle_{T_s} \quad (8)$$

$$i_C(t) = C.\frac{dv(t)}{dt} \approx -\langle i(t)\rangle_{T_s} - \frac{\langle v(t)\rangle_{T_s}}{R} \quad (9)$$

The inductor voltage during the first and second sub-intervals are given by equations (4) and (8) are averaged,

$$\langle v_L(t)\rangle_{T_s} = \frac{1}{T_s}\int_t^{t+T_s} v_L(\tau)d\tau = d(t)\langle v_g(t) - R_L.i(t)\rangle_{T_s} + d'(t)\langle v(t) - R_L.i(t)\rangle_{T_s} \quad (10)$$

Where $d'(t) = 1 - d(t)$

From equation (1),

$$L\frac{d\langle i(t)\rangle_{T_s}}{dt} = d(t)\langle v_g(t)\rangle_{T_s} + d'(t)\langle v(t)\rangle_{T_s} - R_L.\langle i(t)\rangle_{T_s} \quad (11)$$

Averaging methods needs some approximations.

In steady-state, inductor current i(t) is periodic with period equal to the switching period T_s.

$$i(t + T_s) = i(t)$$

During transients, there is a net change in i(t) over one switching period.

$$L\frac{di(t)}{dt} = v_L(t) \quad (12)$$

Divide by L and integrate from "t" to "t+T_s".

$$\int_t^{t+T_s} di = \frac{1}{L}\int_t^{t+T_s} v_L(\tau)d\tau \quad (13)$$

$$\Rightarrow \quad i(t + T_s) - i(t) = \frac{1}{L}.T_s.\langle v_L(t)\rangle_{T_s} \quad (14)$$

Averaging of capacitor waveform can also be done. From equations (5) and (9),

$$\langle i_c(t)\rangle_{T_s} = d(t)\left[-\frac{\langle v(t)\rangle_{T_s}}{R+R_C}\right] + d'(t)\left[-\langle i(t)\rangle_{T_s} - \frac{\langle v(t)\rangle_{T_s}}{R}\right] \quad (15)$$

From equation (1),

$$C\frac{d\langle v(t)\rangle_{T_s}}{dt} = d(t)\left[-\frac{\langle v(t)\rangle_{T_s}}{R+R_C}\right] + d'(t)\left[-\langle i(t)\rangle_{T_s} - \frac{\langle v(t)\rangle_{T_s}}{R}\right] \quad (16)$$

Similarly, averaging for input currents can be done.

$i_g(t)$ =current drawn by converter from input source. By neglecting the inductor current ripple and replacing *i*(*t*) with its averaged value$\langle i(t)\rangle_{T_s}$ we can express the input current as follows:

$$i_g(t) = \begin{cases}\langle i(t)\rangle_{T_s}, & during\ subinterval\ 1\\ 0, & during\ subinterval\ 2\end{cases} \quad (17)$$

upon averaging over one switching period,

$$\langle i_g(t)\rangle_{T_s} = d(t).\langle i(t)\rangle_{T_s} \quad (18)$$

From equations (11),(16) and (18) linearization can be done

$$L\frac{d\langle i(t)\rangle_{T_s}}{dt} = d(t).\langle v_g(t)\rangle_{T_s} + d'(t).\langle v(t)\rangle_{T_s} - R_L.\langle i(t)\rangle_{T_s}$$

$$C\frac{d\langle v(t)\rangle_{T_s}}{dt} = d(t)[-\frac{\langle v(t)\rangle_{T_s}}{R+R_C}] + d'(t)[-\langle i(t)\rangle_{T_s} - \frac{\langle v(t)\rangle_{T_s}}{R}] \quad (19)$$

$$\langle i_g(t)\rangle_{T_s} = d(t).\langle i(t)\rangle_{T_s}$$

Suppose that we drive the converter at some steady-state, or quiescent, duty ratio $d(t) = D$, with quiescent input voltage $v_g(t) = V_g$. From steady-state analysis, after any transients have subsided, the inductor current $\langle i(t)\rangle_{T_s}$, the capacitor voltage $\langle v(t)\rangle_{T_s}$ and the input current $\langle i_g(t)\rangle_{T_s}$ will reach the quiescent values *I*, *V*, and $I_g$respectively, where

$$V = -\frac{D}{D}, V_g \;\&\; I = -\frac{V}{D'R} \;\&\; I_g = DI \quad (20)$$

For small-signal ac model at quiescent operating point (I,V), We assume that the input voltage $v_g(t)$ and duty cycle $d(t)$ are equal to quiescent values V_g and D, plus some small ac variations $\widehat{v_g}(t)$ and $\hat{d}(t)$.

$$\langle v_g(t)\rangle_{T_s} = V_g + \widehat{v_g}(t) \quad (21)$$

$$d(t) = D + \hat{d}(t) \quad (22)$$

In response to these inputs and after any transients have subsided,

$$\langle i(t)\rangle_{T_s} = I + \hat{\imath}(t) \tag{23}$$

$$\langle v(t)\rangle_{T_s} = V + \hat{v}(t) \tag{24}$$

$$\langle i_g(t)\rangle_{T_s} = I_g + \widehat{i_g}(t) \tag{25}$$

With the assumptions that the ac variations arc small in magnitude compared to the dc quiescent values, or

$$\begin{aligned} |\hat{v}_g(t)| &\ll |V_g| \\ |\hat{d}(t)| &\ll |D| \\ |\hat{\imath}(t)| &\ll |I| \\ |\hat{v}(t)| &\ll |V| \end{aligned} \tag{26}$$

The non-linear equation(19) can be linearized by inserting equations (21), (22),(23) & (24) into equation (19).

$$L.\frac{d[I+\hat{\imath}(t)]}{dt} = \left[D + \hat{d}(t)\right].\left[V_g + \hat{v}_g(t)\right] + \left[D' - \hat{d}(t)\right].[V + \hat{v}(t)] - R_L.[I + \hat{\imath}(t)] \tag{27}$$

It should be noted that complement of the duty cycle is given by,

$$d'(t) = [1 - d(t)] = 1 - \left[D + \hat{d}(t)\right] = D' - \hat{d}(t) \tag{28}$$

Where $D' = 1 - D$. By multiplying eqn.(27) and collecting terms,

$$L\left[\frac{dI}{dt} + \frac{d\hat{\imath}(t)}{dt}\right] = \left[DV_g + D'V - R_L.I\right] + \left[D\hat{v}_g(t) + D'\hat{v}(t) + \left(V_g - V\right).\hat{d}(t) - R_L.\hat{\imath}(t)\right] + \hat{d}(t)\left[\hat{v}_g(t) - \hat{v}(t)\right] \tag{29}$$

The derivative of *I* is zero, since *I* is by definition a dc (constant) term. For the purposes of deriving a small-signal ac model, the dc terms can be considered known constant quantities. On the right-hand side of Eq. (25), three types of terms arise:

Dc terms: These terms contain dc quantities only.

First-order ac terms: Each of these terms contains a single ac quantity, usually multiplied by a constant coefficient such as a dc term. These terms are linear functions of the ac variations.

Second-order ac terms: These terms contain the products of ac quantities.

Hence they are nonlinear, because they involve the multiplication of time-varying signals. It is desired to neglect the nonlinear ac terms. Provided that the small-signal assumption, Eq. (22), is satisfied, then each of the second-order nonlinear terms is much smaller in magnitude that one or more of the linear first-order ac terms. We are left with the first-order ac terms on both sides of the equation. Hence,

$$\Rightarrow L\frac{d\hat{\imath}(t)}{dt} = D\hat{v}_g(t) + D'\hat{v}(t) + \left(V_g - V\right)\hat{d}(t) - R_L.\hat{\imath}(t) \tag{30}$$

Insertion of eqn.(22),(23) and (24) into capacitor equation (19) yields,

$$C.\frac{d[V+\hat{v}(t)]}{dt} = \left[-\frac{D.V}{R+R_C} - D'I - D'.\frac{V}{R}\right] + \left[-\frac{D.\hat{v}(t)}{R+R_C} - \frac{\hat{d}(t).V}{R+R_C} + \hat{d}(t).I - D'.\hat{\imath}(t) + \frac{\hat{d}(t).V}{R} - \frac{D'.\hat{v}(t)}{R}\right] + \left[-\frac{\hat{d}(t).\hat{v}(t)}{R+R_C} + \hat{d}(t).\hat{\imath}(t) + \frac{\hat{d}(t).\hat{v}(t)}{R}\right] \tag{31}$$

$$\Rightarrow C\frac{d\hat{v}(t)}{dt} = -\hat{v}(t).\left[\frac{D'}{R} + \frac{D}{R+R_C}\right] + \hat{d}(t).V.\left[\frac{1}{R} - \frac{1}{R+R_C}\right] - D'\hat{\imath}(t) + I.\hat{d}(t) \tag{32}$$

This is the desired small-signal linearized equation that describes variations in the capacitor voltage.

Insertion of equation (22), (23) and (25) into equation (19) yields,

$$I_g + \hat{\imath}_g(t) = \left[D + \hat{d}(t)\right][I + \hat{\imath}(t)] \tag{33}$$

By collecting terms, we obtain

$$I_g + \hat{\imath}_g(t) = (DI) + \left[D\hat{\imath}(t) + I\hat{d}(t)\right] + \hat{d}(t).\hat{\imath}(t)$$

We again neglect the second-order nonlinear terms. The dc terms on both sides of the equation are equal. The remaining first-order linear ac terms are

$$\Rightarrow \hat{\imath}_g(t) = D\hat{\imath}(t) + I\hat{d}(t) \quad (34)$$

The small signal ac description of the buck boost converter with parasitic resistance are collected below:

$$L\frac{d\hat{\imath}(t)}{dt} = D\hat{v}_g(t) + D'\hat{v}(t) + (V_g - V)\hat{d}(t) - R_L.\hat{\imath}(t)$$

$$C\frac{d\hat{v}(t)}{dt} = -\hat{v}(t).\left[\frac{D'}{R} + \frac{D}{R+R_C}\right] + \hat{d}(t).V.\left[\frac{1}{R} - \frac{1}{R+R_C}\right] - D'\hat{\imath}(t) + I.\hat{d}(t)$$

$$\hat{\imath}_g(t) = D\hat{\imath}(t) + I\hat{d}(t)$$

The converter contains two inputs $\hat{d}(s)$ (control input) and $\hat{v}_g(s)$ and one output $\hat{v}(s)$.

Hence,

$$\hat{v}(s) = G_{vd}(s)\hat{d}(s) + G_{vg}(s)\hat{v}_g(s)$$

Where $G_{vd}(s) = \hat{v}(s)/\hat{d}(s)$ when $\hat{v}_g(s) = 0$

$G_{vg}(s) = \hat{v}(s)/\hat{v}_g(s)$ when $\hat{d}(s) = 0$

Here, $G_{vd}(s)$is control-to-Output transfer function.

and $G_{vg}(s)$ is line-to-Output transfer function.

By Laplace transform of converter equations, taking initial conditions as zero

$$sL\hat{\imath}(s) = D\hat{v}_g(s) + D'\hat{v}(s) + (V_g - V)\hat{d}(s) - R_L.i(s)$$

$$sC\hat{v}(s) = -D'\hat{\imath}(s) + I\hat{d}(s) - \hat{v}(s).\frac{(R+D'.R_C)}{R(R+R_C)} + \hat{d}(s).V.\frac{R_C}{R(R+R_C)} \quad (35)$$

Eliminating $\hat{\imath}(s)$ and solving for $\hat{v}(s)$

$$\hat{\imath}(s) = \frac{D\hat{v}_g(s) + D'\hat{v}(s) + (V_g - V).\hat{d}(s)}{sL+R_L} \quad (36)$$

$$\Rightarrow sC.\hat{v}(s) + \hat{v}(s).\frac{(R+D'.R_C)}{R(R+R_C)} = -D'.\hat{\imath}(s) + I.\hat{d}(s) + \hat{d}(s).V.\frac{R_C}{R(R+R_C)} \quad (37)$$

$$\Rightarrow \hat{v}(s).\left[s.C + \frac{R+D'.R_C}{R(R+R_C)} + \frac{D'^2}{s.L+R_L}\right] = -D.\frac{D'}{s.L+R_L}.\hat{v}_g(s) + \left[I + V.\frac{R_C}{R(R+R_C)} - D'.\frac{(V_g-V)}{s.L+R_L}\right].\hat{d}(s) \quad (38)$$

Equation(38) can also be written as,

$$\Rightarrow \hat{v}(s)\left[\frac{A_1.s^2+A_2.s+A_3}{R(R+R_C)(sL+R_L)}\right] = -D.\frac{D'}{s.L+R_L}.\hat{v}_g(s) + \left[\frac{s.B_1+B_2}{R(R+R_C)(sL+R_L)}\right].\hat{d}(s) \quad (39)$$

Where

$$A_1 = (R+R_C).CRL \quad (40)$$

$$A_2 = L(R + D'.R_C) + CRR_L(R+R_C) \quad (41)$$

$$A_3 = D'^2.R(R+R_C) + D'.R_CR_L + RR_L \quad (42)$$

$$B_1 = IRL(R+R_C) + VR_CL \quad (43)$$

$$B_2 = IRR_L(R+R_C) + VR_CR_L - D'(V_g - V).R(R+R_C) \quad (44)$$

$$\Rightarrow \hat{v}(s) = \left[-\frac{DD'.R(R+R_C)}{A_1.s^2+A_2.s+A_3}\right].\hat{v}_g(s) + \left[\frac{B_1.s+B_2}{A_1.s^2+A_2.s+A_3}\right].\hat{d}(s) \quad (45)$$

Which is of the form

$$\hat{v}(s) = G_{vd}(s)\hat{d}(s) + G_{vg}(s)\hat{v}_g(s)$$

Hence, control to output transfer function and line-to-output transfer function can be derived as

$$G_{vd}(s) = \frac{B_1.s+B_2}{A_1.s^2+A_2.s+A_3} \quad (46)$$

$$G_{vg}(s) = -\frac{DD'.R(R+R_C)}{A_1.s^2+A_2.s+A_3} \quad (47)$$

Values of A_1, A_2, A_3, B_1 and B_2 can be calculated with the help of equations (40), (41), (42), (43) and (44) respectively.

3. Closed Loop Transfer Function of Buck Boost Converter Based Control System

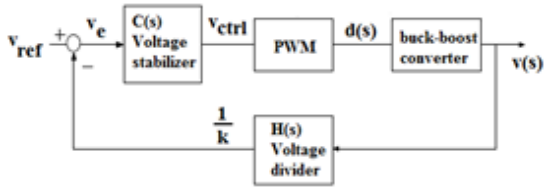

Figure 5. Block Diagram of closed loop buck boost converter based control system

From the above block diagram, it can be written as,

$$\hat{v}_e = V_{ref} - H(s).\hat{v}(s) \quad (48)$$

$$\hat{v}_{ctrol} = C(s).\hat{v}_e \quad .(49)$$

$$\hat{d}(s) = \hat{v}_{ctrol}.\frac{1}{V_P} \quad (50)$$

$$\hat{v}(s) = \hat{d}(s).G_{vd}(s) \quad (51)$$

Hence, From above equations,

$$\hat{v}(s) = C(s)\left[V_{ref} - H(s).\hat{v}(s)\right].\frac{1}{V_P}.G_{vd}(s)$$

$$\Rightarrow \frac{\hat{v}(s)}{V_{ref}} = \frac{C(s).G_{vd}(s)}{V_P + C(s).H(s).G_{vd}(s)} \quad (52)$$

Equation (52) shows the closed loop transfer function of the buck-boost converter. Here, $C(s)$ is the transfer function of Voltage Stabilize. $H(s)$ is the transfer function of Voltage divider.

$\frac{1}{V_P}$ is the transfer function of PWM.

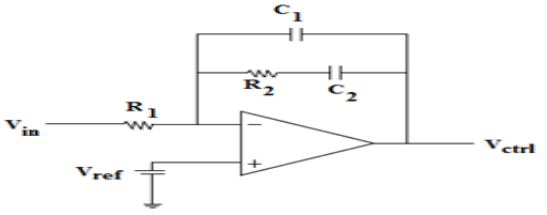

Figure 6. Control circuit for the system

$$C(s) = \frac{1}{R_1.C_1}.\frac{s+\frac{1}{R_2.C_2}}{s\left(s+\frac{C_1+C_2}{R_1C_1.C_2}\right)} \quad (53)$$

Take, $H(s) = \frac{1}{K}$ (54)

Hence,

$$\frac{\hat{v}(s)}{V_{ref}} = \frac{K[B_1R_2C_2.s^2+(B_1+B_2R_2C_2).s+B_2]}{Q_4.s^4+Q_3.s^3+Q_2.s^2+Q_1.s+1} \quad (55)$$

In equation(55),

$$Q_4 = V_P.K.R_1R_2C_1C_2.A_1 \quad (56)$$

$$Q_3 = V_P.K[A_2R_1R_2C_1C_2 + A_1(C_1+C_2)R_2] \quad (57)$$

$$Q_2 = V_P.K[A_3R_1R_2C_1C_2 + A_2(C_1+C_2)R_2] \quad (58)$$

$$Q_1 = V_P.K.A_3(C_1+C_2).R_2 + R_2.C_2 \quad (59)$$

4. Result and Discussion

Table 1:

parameter	value	parameter	value
R	2.4 ohms	R_L	5 ohm
L	0.01H	R_C	5 ohm
C	0.5 F	C_3	81.1058mF
V_{in}	8 V	V_o	12 V
Duty ratio	0.6	R_2	2.86726ohms

Based on the parameter of different components as mentioned in table1 the transfer function of converter and overall system has been calculated and bode plot has been plotted by using MATLAB. In the other way depending upon the nature of regulator and type of converter the transfer function has been obtained by PSIM .Finally, the performance of regulator ,converter and overall system has been observed as stable. Figure 7 to Figure 12 shows the nature of bode plot obtained with the help of MATLAB and PSIM.

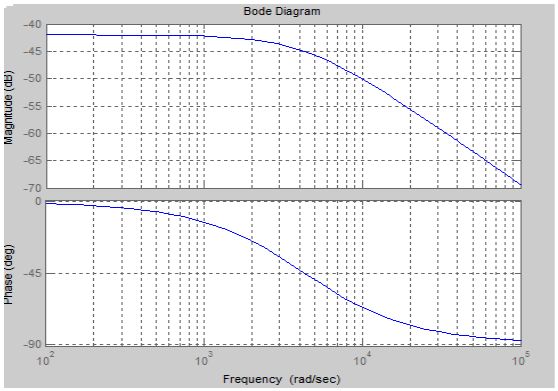

Figure7. Bode plot of regulator by MATLAB

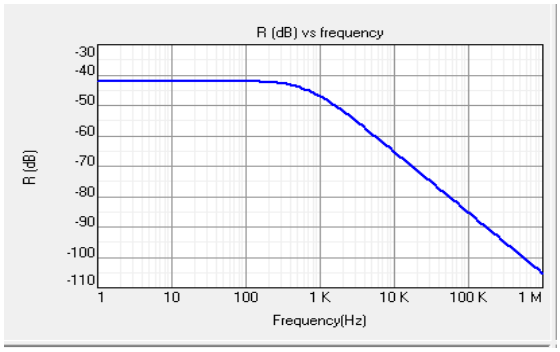

Figure8. Bode plot (magnitude) of regulator by PSIM

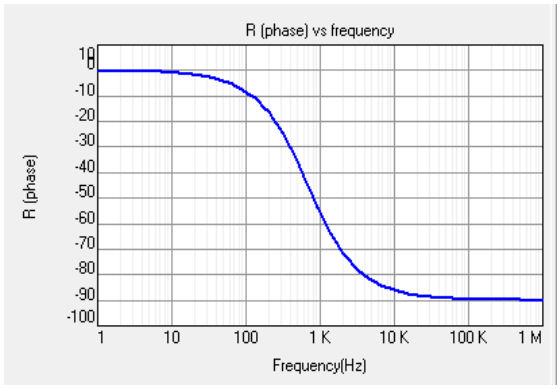

Figure 9. Bode plot (phase) of regulator by PSIM

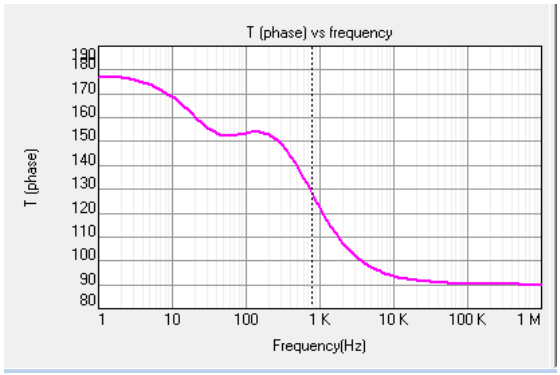

Figure 10. Bode plot(phase) of overall transfer function by PSIM

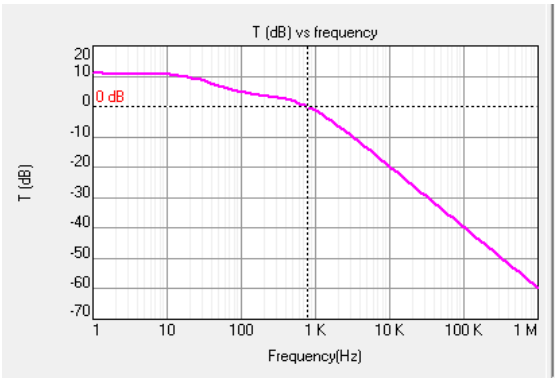

Figure 11. Bode plot (magnitude) of overall transfer function by PSIM

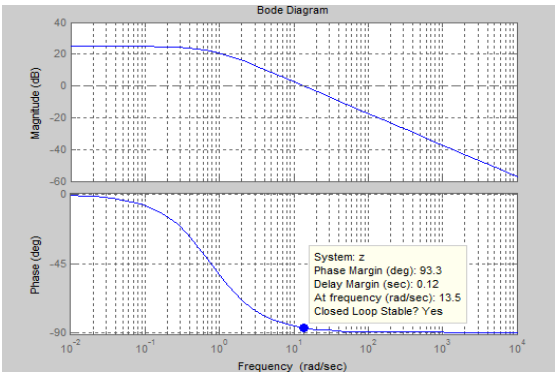

Figure12. Bode plot of overall transfer function by MATLAB

Figure 13. Output Current waveform.

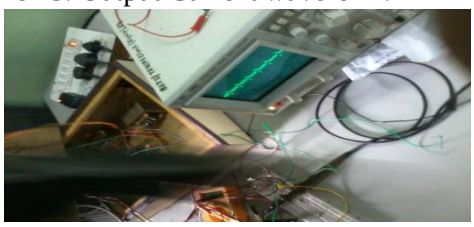

Figure 14. Output Current with sudden change in load.

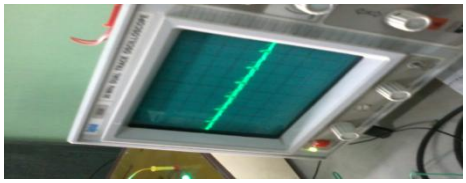

Figure 15. Output Current with sudden change in supply voltage.

5. Prototype Developments

It is observed that for a load of 20 Ohms, a constant current of 600mA is obtained. Fig. 13 shows the constant current waveform while Fig. 14 shows current with sudden change in load and Fig. 15 shows current with sudden change in supply voltage. The prototype for buck boost switch based closed loop has been designed for a power rating of 10W with 10V output at 100 KHz switching frequency in CCM operation using microcontroller IC number 8951 based PWM and efficiency has been obtained as 80% with ripple value of 0.02%. The system has been tested for 20% change of load. The system has been tested for 12 hours to check the performance of the system.

6. Conclusion

Based on the result obtained from the system it has been observed that LED has been illuminated for constant intensity. The phase margin of the buck boost converter and whole driver circuit has been observed as 93.206º and 93.8º respectively making system as stable and suitable for typical environmental scenario.

References

[1] V. von Kaenel, P. Macken, and M. G. R. Degrauwe, "A Voltage Reduction Technique for Battery-Operated Systems," IEEE Journal of Solid- State Circuits, vol.25, no. 5, pp. 1136–1140, Oct. 1990

[2] H. J. Chiu and S. J. Cheng, "Led backlight driving system for large-scale lcd panels," IEEE Transactions on Industrial Electronics, vol. 54, no. 5, pp. 2751-2760, Oct. 2007.

[3] Y. H. Fan et al., "A simplified led converter design and implement," Joint Conference on Information Sciences, pp. 8-11, Oct. 2006.

[4] Philips Electronics, part number LXCL-PWF3, Power light source LUXEON Flash.

[5]] V. von Kaenel, M. Pardoen, E. Dijkstra, and E. Vittoz, "Automatic Adjustment of Threshold and Supply Voltages for Minimum Power Consumption in CMOS Digital Circuits," in IEEE Symposium on Low Power Electronics, Digest of Technical Papers, Oct. 10–12, 1994, pp. 78-79.

[6]. T. Wang, X. Zhou, and F. Lee, "A Low Voltage High Efficiency and High Power Density DC/DC Converter," in 28th Annual IEEE Power Electronics Specialists Conference, PESC 1997, vol. 1, Jun. 22–27, 1997, pp. 240–245.

[7]. F. S. Kang, S. J. Park, and C. U. Kim, "ZVZCS single-stage PFC AC to-DC half-bridge converter," IEEE Trans. Ind. Electron., vol. 49, no. 1, pp. 206–216, Feb. 2002.

[8]. Huang-Jen Chiu, et al, LED Backlight Driving System for Large-Scale LCD Panels, IEEE Trans on Industrial Electronics, Vol.54, No.5, 2007, pp2751-2769.

[9]. Z. Ye, Fred Greenfeld, George Liang, Design consideration of SEPIC converters for high brightness LED applications, IEEE PESC 2008, June 2008, Greece, pp 2657-2663.

[10]. R. Cope and Y. Podrazhansky, "The Art of Battery Charging," in 14th Annual Battery Conference on Applications and Advances, Jan. 12–15, 1999, pp. 233–235.

[11]. Clauberg et al., Light Emitting Diode Driver, United State Patent US 6,853,150 B2, February 2005.

[12]. Manuel Rico-Secades, Antonio J. Calleja, et al, Evaluation of a Low-Cost Permanent Emergency Lighting System Based on High-Efficiency LEDs, IEEE Trans on Industry Applications, Vol. 41, NO. 5, Sept/Oct 2005, pp1386-1390. 11.

[13] R.P.Gupta, U Prasad, P.K.Sadhu and N.pal " Efficient Lighting System for Underground Coalmines Using LED" Page 21-24 Volume 91, August, 2010, Journal of The Institution of Engineers(India)-MN.

[14] Chi-Jen Huang; Ying-Chun Chuang; Yu-Lung Ke; " Design of Closed-loop Buck-boost Converter for LED Driver Circuit" Industrial and Commercial Power Systems Technical Conference (I&CPS), 2011 IEEE PP-1 – 6, Baltimore, MD ,1-5 May 2011

Ramjee Prasad Gupta is a member of faculty at Department of Electrical Engineering , BIT, Sindri. His research interest include PWM based energy efficient lighting system and stability analysis of power system.

Dibya Bharti is currently working towards the MTech degree in Power system at BIT, Sindri. Her research interest include efficient converter for low power application and harmonic analysis in power supply.

Dr. Upendra Prasad is a member of faculty at Department of Electrical Engineering , BIT, Sindri. His research interest include power quality and reliability analysis.